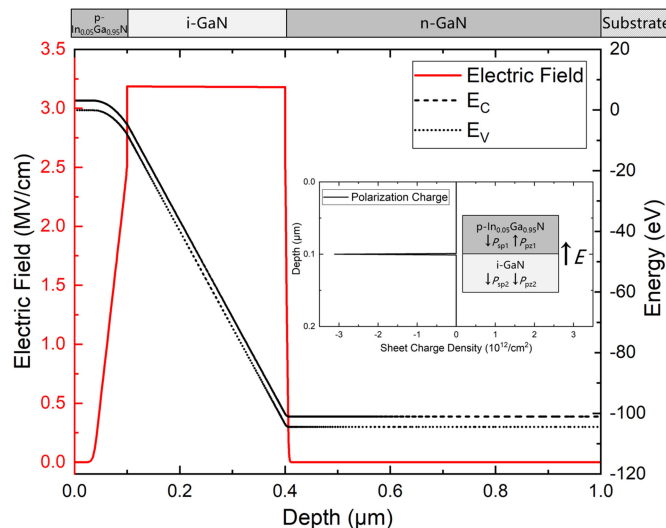


Polarization Enhanced GaN Avalanche Photodiodes With p-type $\text{In}_{0.05}\text{Ga}_{0.95}\text{N}$ Layer

Volume 12, Number 1, February 2020

Haiping Wang
Haifan You
Danfeng Pan
Dunjun Chen
Hai Lu
Rong Zhang
Youdou Zheng



DOI: 10.1109/JPHOT.2020.2969991

Polarization Enhanced GaN Avalanche Photodiodes With p-type $\text{In}_{0.05}\text{Ga}_{0.95}\text{N}$ Layer

Haiping Wang, Haifan You , Danfeng Pan, Dunjun Chen, Hai Lu , Rong Zhang, and Youdou Zheng

Key Laboratory of Advanced Photonic and Electronic Materials, School of Electronic Science and Engineering, Collaborative Innovation Center of Advanced Microstructures, Nanjing University, Nanjing 210093, China

DOI:10.1109/JPHOT.2020.2969991

This work is licensed under a Creative Commons Attribution 4.0 License. For more information, see <http://creativecommons.org/licenses/by/4.0/>

Manuscript received November 29, 2019; revised January 19, 2020; accepted January 22, 2020. Date of publication January 28, 2020; date of current version February 24, 2020. This work was supported in part by the National Key R&D Program of China under Grant 2016YFB0400903, in part by the NSFC under Grant 61634002, in part by the NSAF under Grant U1830109, in part by the "333" project of Jiangsu Province, China under Grant BRA2018040, and in part by the Natural Science Foundation of Jiangsu Province under Grant BK20180327. Corresponding authors: Danfeng Pan; Dunjun Chen (e-mail: pdf@nju.edu.cn; djchen@nju.edu.cn).

Abstract: In this letter, novel heterostructure p-i-n GaN avalanche photodiodes (APDs) with p-type $\text{In}_{0.05}\text{Ga}_{0.95}\text{N}$ layer are proposed and analyzed through Silvaco Atlas simulations. The introduction of the $\text{In}_{0.05}\text{Ga}_{0.95}\text{N}$ layer generates a negative polarization charge at the p- $\text{In}_{0.05}\text{Ga}_{0.95}\text{N}$ /i-GaN heterojunction interface via the piezoelectric polarization effect. Three times higher hole concentration in the p- $\text{In}_{0.05}\text{Ga}_{0.95}\text{N}$ layer is obtained due to the smaller activation energy of the Mg dopant. Induced polarization charge and increased hole concentration work together to reduce the voltage drop in the p- $\text{In}_{0.05}\text{Ga}_{0.95}\text{N}$ layer and enhance the electric field intensity in the i-GaN layer. The calculated results show that the heterostructure APD demonstrates a reduced operating voltage of more than 26 V and an improved multiplication gain by an order of magnitude in comparison to the conventional one.

Index Terms: GaN, avalanche photodiodes, p-type $\text{In}_{0.05}\text{Ga}_{0.95}\text{N}$, polarization, hole concentration, Silvaco, simulation.

1. Introduction

Avalanche photodiodes (APDs) based on III-nitride are attracting great attention due to their capabilities of low dark-current density, large optical gain as well as Geiger-mode operation [1], [2]. In addition, III-nitride APDs provide natural filters with tunable cutoff wavelengths for high-sensitivity visible- or solar-blind ultraviolet (UV) detection [3], [4]. Compared to photomultiplier tubes (PMTs) that are bulky, fragile, and require optical filters, GaN-based UV-APDs show excellent potential for numerous applications in military systems, medical systems, imaging systems, and space research [5].

GaN-based UV-APDs require a voltage over 100 V to achieve high sensitivity and large internal gain in Geiger-mode operation. High operation voltage, however, results in electric field crowding at the contact and mesa edges, leading to increased leakage current and microplasma breakdown [6]. To reduce the device operating voltage, the voltage drop in n and p-type contact layers should be minimized with carrier concentrations as high as possible. However, GaN is suffering

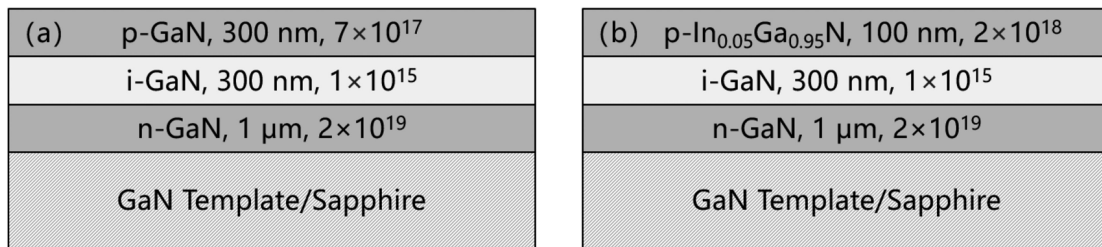


Fig. 1. Schematic structures of the (a) conventional and (b) heterostructure p-i-n GaN APDs.

from relatively low p-type doping efficiency due to the high Mg-acceptor activation energy [7]. Additionally, increasing dopant incorporation in p-type GaN beyond a certain value can lead to the development of stress and formation of defects, which further degrades device performance.

In this work, a novel p-i-n GaN-based APD with the replacement of the p-GaN layer by the p-In_{0.05}Ga_{0.95}N layer is proposed. With a narrower bandgap, the p-In_{0.05}Ga_{0.95}N layer exhibits a relatively smaller Mg activation energy and yields several times higher hole concentration under the same Mg doping concentration [8]–[11]. The Negative polarization sheet charge is induced at the interface of p-In_{0.05}Ga_{0.95}N/i-GaN heterojunction via piezoelectric polarization [12], [13]. Two-dimensional (2-D) numerical simulations are carried out to illustrate the effects of polarization engineering and hole concentration on the performance of GaN APDs. The electric field intensities, breakdown voltages, multiplication gains, and spectral responses of both the conventional and heterostructure GaN APDs are studied in detail.

2. Device Structure and Simulation Models

Fig. 1 plots the schematic (cross-sectional) structures of the conventional and heterostructure p-i-n GaN APDs. The conventional structure consists of a 1- μ m-thick heavily doped n-type GaN layer ($n \sim 2 \times 10^{19} \text{ cm}^{-3}$), a 300-nm-thick unintentional doped GaN layer ($n \sim 1 \times 10^{15} \text{ cm}^{-3}$), and a 300-nm-thick p-type GaN layer ($p \sim 7 \times 10^{17} \text{ cm}^{-3}$) from bottom to top. The heterostructure APD is similar to the conventional one except for the p-In_{0.05}Ga_{0.95}N layer. According to [10], under the same Mg doping concentration ($4 \times 10^{19} \text{ cm}^{-3}$), the hole concentration of p-In_{0.05}Ga_{0.95}N ($2 \times 10^{18} \text{ cm}^{-3}$) is approximately three times higher than that of p-GaN. The relatively thinner p-In_{0.05}Ga_{0.95}N layer (100 nm) is attributed to the rapid decrease of electric field intensity within it, which will be discussed later.

Steady-state 2-D numerical simulations based on Silvaco Atlas software are performed. Fundamental equations consist of Poisson's Equation, the continuity equations, and the transport equations. The physical models can be grouped into five classes: Carrier Statistics Models (boltzmann), Mobility Models (fldmob), Carrier Generation-Recombination Models (SRH, optr, and auger), Band-to-Band Tunneling Models (bbt.std), and Impact Ionization Models (selb). Polarization Model (polariz) which is critical for wurtzite materials is also enabled.

The effective density of states, saturation velocities, and BBT coefficients are extracted from [14]. The impact ionization coefficients are extracted from [15]. The refractive index n and extinction coefficient k of GaN and In_{0.05}Ga_{0.95}N are extracted from [16] and [17], respectively. The electron and hole lifetimes, auger coefficients, conduction band alignment, and density of trap centers are extracted from our previous work [12], [18]. The polarization scale factor is assumed to be 0.6.

3. Results and Discussions

Fig. 2 demonstrates the dark current, photocurrent, and avalanche gain for the conventional and heterostructure APDs as a function of reverse bias. The avalanche gain (M) is calculated as the difference between the multiplied photocurrent and dark current, normalized by the difference

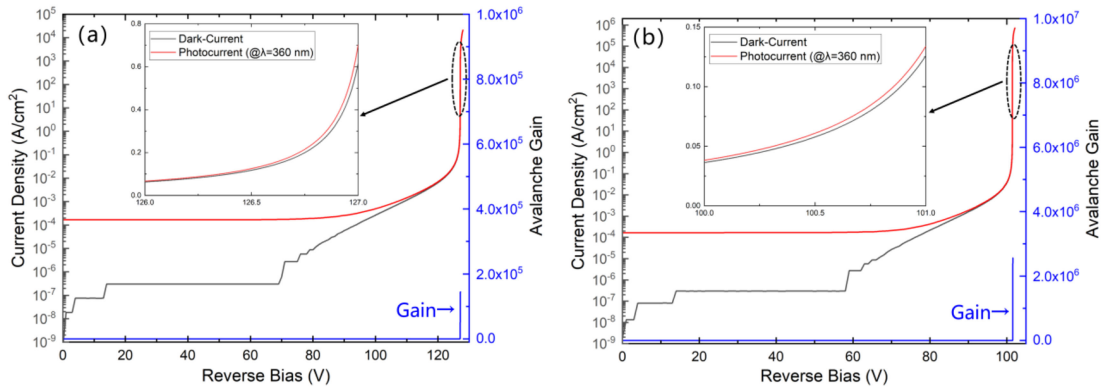


Fig. 2. Dark current, photocurrent, and avalanche gain of the (a) conventional and (b) heterostructure APDs versus reverse bias.

between the unmultiplied photocurrent and dark current. The unmultiplied currents are taken from the flat region of the I-V plots at 50 V reverse bias. To obtain the photocurrent distributions, UV light at the 360 nm visible-blind wavelength with an optical intensity of $1 \times 10^{-2} \text{ W/cm}^2$ was used to illuminate the front surfaces of the APDs.

Under dark conditions, the conventional APD maintains a low leakage current density below a reverse voltage of 70 V, as plotted in Fig. 2(a). Above 70 V, the dark current grows monotonically, indicating increased generation current from the bulk space-charge region. Beyond 125 V, the dark current rose sharply, suggesting an active impact ionization in the multiplication region. Under illumination, the photocurrent remains constant until the reverse bias of 70 V and then increases dramatically, where the impact ionization process starts to dominate the current. During the avalanche multiplication process, the photocurrent rose noticeably over the dark current background (see Fig. 2(a), inset) and the maximum avalanche gain calculated is 2×10^5 at the breakdown voltage (V_{BR}) of 127.2 V.

The I-V characteristics of the heterostructure APD are likewise the case for the conventional one, as shown in Fig. 2(b). The multiplication process, however, starts at a lower reverse bias of ~ 100 V. Beyond the voltage of 101 V, the avalanche current reaches a value of $1 \times 10^6 \text{ A/cm}^2$ and the avalanche gain exceeds 2×10^6 , both an order of magnitude higher than those of the conventional one. The enhanced avalanche current and gain imply that the device underwent a stronger multiplication process above the onset point.

Fig. 3 presents the simulated band diagrams and electric field profiles of the conventional and heterostructure APDs at the voltage point with the maximum multiplication gain. The conventional APD in Fig. 3(a) requires an operating voltage of 127 V to achieve the critical electric field ($\sim 3.2 \text{ MV/cm}$) in the multiplication region. A voltage drop of 34.88 V is seen in the p-GaN layer whereas a drop of 1.08 V is shown in the n-GaN region. As to the heterostructure APD, the corresponding voltage drops in p-In_{0.05}Ga_{0.95}N and n-GaN layers are merely 7.90 V and 0.96 V respectively, indicating a significant reduction of voltage drop for more than 26 V in p-type layer. As a consequence, 101 V is enough for the avalanche process.

The effects of polarization engineering (PE) and hole concentration (HC) on the electric field distribution and voltage drop in the p-In_{0.05}Ga_{0.95}N layer are investigated one by one in Fig. 4. The profile in the p-GaN layer is also exhibited at the voltage point of 50 V as a reference. To shed light on the effect of polarization engineering, hole concentration in the p-In_{0.05}Ga_{0.95}N layer was set the same as in the p-GaN layer ($p \sim 7 \times 10^{17} \text{ cm}^{-3}$), as presented in the blue shot dot line. At the heterojunction interface of the p-In_{0.05}Ga_{0.95}N/i-GaN layer, a negative sheet charge of $3 \times 10^{12} \text{ cm}^{-2}$ is induced due to the piezoelectric polarization effect [19], as shown in the inset of Fig. 4. The fixed negative charge results in the polarization electric field, which serves to steeply decrease the electric field intensity in the p-In_{0.05}Ga_{0.95}N layer within a very small distance.

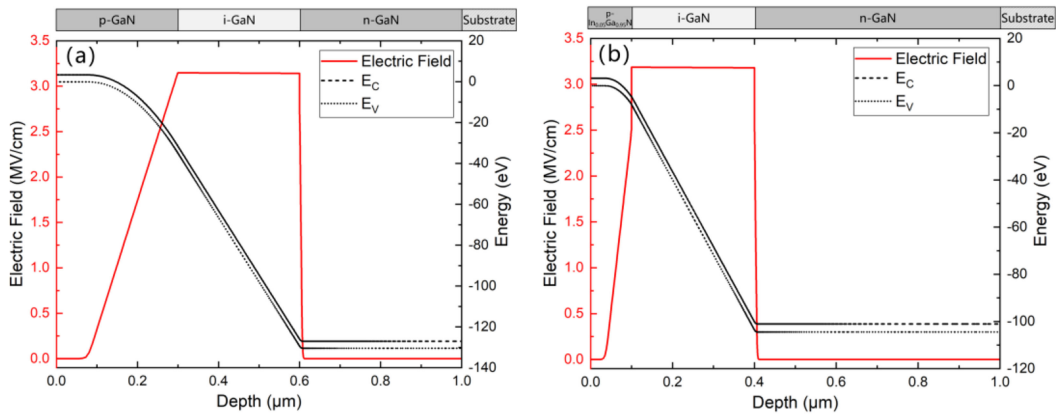


Fig. 3. Structure, band diagram, and electric field distribution of the (a) conventional and (b) heterostructure APDs at the voltage point of 127 V and 101 V, respectively.

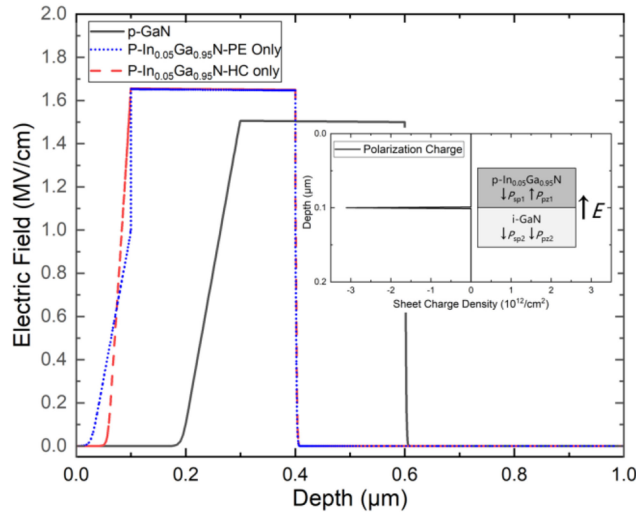


Fig. 4. Electric field profiles of the conventional and heterostructure APDs under the reverse bias of 50 V. Inset is the polarization charge distribution at p-In_{0.05}Ga_{0.95}N/i-GaN interface.

The voltage drop in the p-In_{0.05}Ga_{0.95}N layer reduces to only 3.61 V compared to 8.07 V in the p-GaN layer. To investigate the influence of hole concentration, the piezoelectric polarization effect was not taken into account in the heterostructure APD, as plotted in the red dash line. Owing to the three times higher hole concentration, the p-In_{0.05}Ga_{0.95}N layer exhibits steep and uniform descent of the electric field, with a voltage drop of only 3.48 V.

As observed, polarization engineering and hole concentration act independently in the regulation of the electric field, but their effects are superimposable. The induced negative charge and increased hole concentration both contribute to the rapid decrease of electric field intensity and the significant reduction of voltage drop in the p-In_{0.05}Ga_{0.95}N layer. Therefore, the i-GaN layer in the heterostructure APD undertakes greater voltage drop and demonstrates enhanced electric field intensity, which results in reduced operating voltage and resultant improved avalanche performance. The rapid decrease of electric field intensity also allows for a relatively thin p-In_{0.05}Ga_{0.95}N layer, which avoids additional absorption loss and enables the frontside illumination geometry.

Fig. 5(a) presents the reverse bias dependent spectral response of the conventional APD as a function of wavelength. The responsivity reaches a maximum value of 271.6 mA/W at 360 nm under

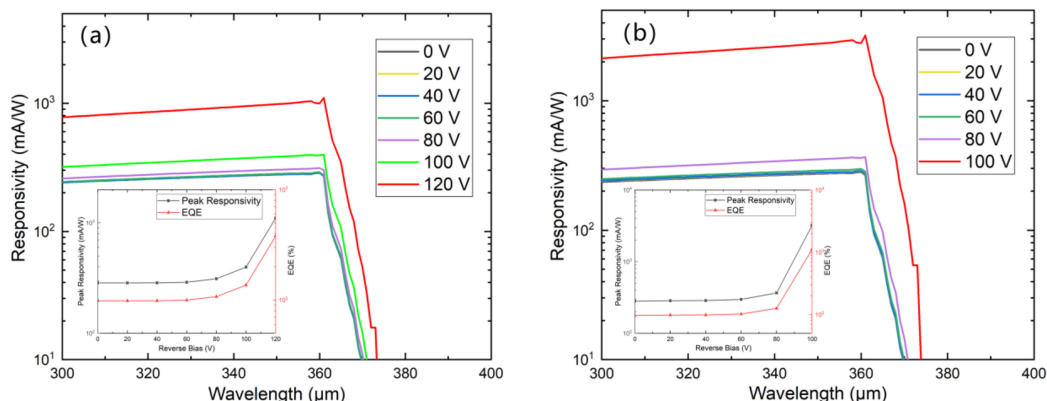


Fig. 5. Reverse bias dependent spectral response of the (a) conventional and (b) heterostructure APDs. Inset is the relationship between peak responsivity, EQE and reverse bias.

zero bias, corresponding to an external quantum efficiency (EQE) of 93.6%. The peak responsivity and EQE remain constant below the reverse bias of 80 V, and then increase exponentially with the elevated bias, as plotted in the inset of Fig. 5(a). At a reverse bias of 100 V, the EQE at 361 nm exceeds 100%, indicating the start of an avalanche process. At a reverse bias of 120 V closer to the breakdown voltage, the peak responsivity increases to 949.8 mA/W at 361 nm, corresponding to an EQE of 327.1%. The significant rise in the responsivity is determined to be the result of carrier impact ionization approaching the onset of avalanche multiplication.

The responsivity curves for the heterostructure APD are given in Fig. 5(b), which is likewise the case for the conventional one. No additional absorption loss is observed owing to the relatively thin p-In_{0.05}Ga_{0.95}N layer, as analyzed previously. Meanwhile, the heterostructure APD exhibits a much higher peak responsivity (3044.6 mA/W at 361 nm) at a lower value of reverse bias (100 V). The calculated EQE (913.7%) increases by a factor of three compared to the conventional structure, which is related to the enhanced electric field intensity in the i-GaN layer.

4. Conclusion

In this letter, a novel heterostructure p-i-n GaN APD with p-In_{0.05}Ga_{0.95}N layer was proposed and analyzed through Silvaco based 2-D numerical simulations. The negative polarization sheet charge of $3 \times 10^{12} \text{ cm}^{-2}$ is induced at the interface of In_{0.05}Ga_{0.95}N/GaN heterojunction via the piezoelectric polarization effect. Three times higher hole concentration in the p-In_{0.05}Ga_{0.95}N layer is obtained due to the smaller activation energy of the Mg dopant. Induced polarization charge and increased hole concentration work together to reduce the voltage drop in the p-In_{0.05}Ga_{0.95}N layer and enhance the electric field intensity in the i-GaN layer. As a result, the heterostructure APD demonstrates a reduced operating voltage of more than 26 V and an improved multiplication gain by an order of magnitude in comparison to the conventional one. Additionally, the relatively thin p-In_{0.05}Ga_{0.95}N layer avoids deadweight photon loss and maintains frontside illumination geometry with higher external quantum efficiency. The application of p-type InGaN presented here is in the context of visible-blind GaN p-i-n APD and can be extended to solar-blind AlGaIn APDs.

References

- [1] M. H. Ji *et al.*, "Uniform and reliable GaN p-i-n ultraviolet avalanche photodiode arrays," *IEEE Photon. Technol. Lett.*, vol. 28, no. 19, pp. 2015–2018, Oct. 2016.
- [2] M. H. Ji, J. Kim, T. Detchprohm, Y. Z. Zhu, S. C. Shen, and R. D. Dupuis, "p-i-p-i-n separate absorption and multiplication ultraviolet avalanche photodiodes," *IEEE Photon. Technol. Lett.*, vol. 30, no. 2, pp. 181–184, Jan. 2018.

- [3] Z. G. Shao *et al.*, "High-gain AlGaIn solar-blind avalanche photodiodes," *IEEE Electron Device Lett.*, vol. 35, no. 3, pp. 372–374, Mar. 2014.
- [4] Z. G. Shao *et al.*, "Ionization-enhanced AlGaIn heterostructure avalanche photodiodes," *IEEE Electron Device Lett.*, vol. 38, no. 4, pp. 485–488, Apr. 2017.
- [5] A. K. Sood *et al.*, "Development of high gain GaN/AlGaIn avalanche photodiode arrays for UV detection and imaging applications," *Int. J. Eng.*, vol. 10, no. 2, pp. 129–150, 2017.
- [6] J. Bulmer *et al.*, "Visible-blind APD heterostructure design with superior field confinement and low operating voltage," *IEEE Photon. Technol. Lett.*, vol. 28, no. 1, pp. 39–42, Jan. 2016.
- [7] C. C. Yu, C. F. Chu, J. Y. Tsai, C. F. Lin, and S. C. Wang, "Electrical and optical properties of beryllium-implanted Mg-doped GaN," *J. Appl. Phys.*, vol. 92, no. 4, pp. 1881–1887, Aug. 2002.
- [8] K. Kumakura, T. Makimoto, and N. Kobayashi, "Activation energy and electrical activity of Mg in Mg-doped In_xGa_{1-x}N ($x < 0.2$)," *Jpn. J. Appl. Phys. 2*, vol. 39, no. 4b, pp. L337–L339, Apr. 2000.
- [9] S. N. Lee *et al.*, "Investigation of optical and electrical properties of Mg-doped p-In_xGa_{1-x}N, p-GaN and p-Al_yGa_{1-y}N grown by MOCVD," *J. Cryst. Growth*, vol. 272, no. 1–4, pp. 455–459, Dec. 2004.
- [10] D. Iida, M. Iwaya, S. Kamiyama, H. Amano, and I. Akasaki, "High hole concentration in Mg-doped a-plane Ga_{1-x}In_xN ($0 < x < 0.30$) grown on r-plane sapphire substrate by metalorganic vapor phase epitaxy," *Appl. Phys. Lett.*, vol. 93, no. 18, Nov. 2008, Art. no. 182108.
- [11] B. N. Pantha, A. Sedhain, J. Li, J. Y. Lin, and H. X. Jiang, "Electrical and optical properties of p-type InGaIn," *Appl. Phys. Lett.*, vol. 95, no. 26, Dec. 2009, Art. no. 261904.
- [12] K. X. Dong *et al.*, "Exploitation of polarization in back-illuminated AlGaIn avalanche photodiodes," *IEEE Photon. Technol. Lett.*, vol. 25, no. 15, pp. 1510–1513, Aug. 2013.
- [13] Z. G. Shao *et al.*, "Significant performance improvement in AlGaIn solar-blind avalanche photodiodes by exploiting the built-in polarization electric field," *IEEE J. Sel. Topics Quantum Electron.*, vol. 20, no. 6, pp. 187–192, Nov.-Dec. 2014.
- [14] X. D. Wang *et al.*, "Study of gain and photoresponse characteristics for back-illuminated separate absorption and multiplication GaN avalanche photodiodes," *J. Appl. Phys.*, vol. 115, no. 1, Jan. 2014, Art. no. 013103.
- [15] L. Cao *et al.*, "Experimental characterization of impact ionization coefficients for electrons and holes in GaN grown on bulk GaN substrates," *Appl. Phys. Lett.*, vol. 112, no. 26, Jun. 2018, Art. no. 262103.
- [16] G. Yu *et al.*, "Optical properties of Al_xGa_{1-x}N/GaN heterostructures on sapphire by spectroscopic ellipsometry," *Appl. Phys. Lett.*, vol. 72, no. 18, pp. 2202–2204, May 1998.
- [17] R. Goldhahn *et al.*, "Determination of optical constants for cubic In_xGa_{1-x}N layers," *Physica Status Solidi B-Basic Solid State Phys.*, vol. 216, no. 1, pp. 265–268, Nov. 1999.
- [18] H. F. You *et al.*, "Fine control of the electric field distribution in the heterostructure multiplication region of AlGaIn avalanche photodiodes," *IEEE Photon. J.*, vol. 9, no. 3, Jun. 2017, Art. no. 6802007.
- [19] O. Ambacher *et al.*, "Two dimensional electron gases induced by spontaneous and piezoelectric polarization in undoped and doped AlGaIn/GaN heterostructures," *J. Appl. Phys.*, vol. 87, no. 1, pp. 334–344, Jan. 2000.